

Article:

Azizi, Kolsoom; Moraveji, Mostafa Keshavarz; Arregi, Aitor; Amutio, Mainer; Lopez, Gartzten; Olazar, Martin. **On the pyrolysis of different microalgae species in a conical spouted bed reactor: Bio-fuel yields and characterization.** *Bioresource Technology* 311: 123561 (2020)

Received 20 February 2020; Received in revised form 26 April 2020; Accepted 27 April 2020 Available online 20 May 2020

This work is made available online in accordance with publisher policies. To see the final version of this work please visit the publisher's website. Access to the published online version may require a subscription. Link to publisher's version:

<https://doi.org/10.1016/j.biortech.2020.123561>

Copyright statement:

© 2020 Elsevier B.V. Full-text reproduced in accordance with the publisher's self-archiving policy. This manuscript version is made available under the CC-BY-NC-ND 4.0 license

<http://creativecommons.org/licenses/by-nc-nd/4.0/>



1
2
3
4 **On the pyrolysis of different microalgae species in a conical spouted bed reactor: bio-fuel**
5
6 **yields and characterization**
7

8
9 Kolsoom Azizi^a, Mostafa Keshavarz Moraveji^{a*}, Aitor Arregi^b, Maider Amutio^b, Gartzzen
10
11 Lopez^{b,c}, Martin Olazar^b
12

13
14 ^aDepartment of Chemical Engineering, Amirkabir University of Technology (Tehran
15
16 Polytechnic), 424 Hafez Avenue, Tehran, 1591634311, Iran
17

18
19 ^bDepartment of Chemical Engineering, University of the Basque Country, P.O. Box 644,
20
21 E48080, Bilbao, Spain
22

23
24 ^cIKERBASQUE, Basque Foundation for Science, Bilbao, Spain
25

26
27 Email: moraveji@aut.ac.ir, Phone: +982164543182
28

29 **Abstract**
30

31 The aim of this work was to study fast pyrolysis of three microalgae species in a continuous
32
33 bench-scale conical spouted bed reactor at 500°C. Bio-gas, bio-oil and bio-char yields have been
34
35 determined and characterized by using GC, GC/MS, elemental analyzer and SEM. Bio-oil was
36
37 the main product obtained through pyrolysis of microalgae. The non-condensable gaseous stream
38
39 is made up of mainly hydrogen, carbon monoxide and carbon dioxide, apart from other light
40
41 hydrocarbons detected in lower concentration, as are methane, ethane, ethylene, propane and
42
43 propylene. The compounds identified in the bio-oil have been categorized into hydrocarbons,
44
45 nitrogen containing compounds, ketones, alcohols, acids, lactones, phenols and aldehydes. The
46
47 nitrogen and carbon contents of the microalgae bio-chars are higher than those for bio-chars
48
49 derived from other biomasses. Pyrolysis improved the morphology and porous structure of
50
51 microalgae. Finally, the mechanism involving microalgae pyrolysis has been approached and the
52
53 main reaction pathways have been proposed.
54
55
56
57
58
59
60
61
62
63
64
65

1
2
3
4 **Keywords:** Pyrolysis; Conical spouted bed; Biomass; Microalgae; Bio-fuel; Kinetic pathway
5
6

7 **1. Introduction**

8
9 Renewable energy sources are becoming an alternative to fossil fuels due to the depletion of
10 fossil fuels and their environmental effects, such as global warming, and air and water pollution.
11

12 Besides, the growth of the world population increases the global energy demand steadily. A
13 practical solution to the mentioned problems is to seek alternative fuels that are green and
14 sustainable. Microalgae have been considered as one of the most promising alternative resources
15 for the production of 3rd generation of bio-fuels due to their high potential for biomass
16 production, efficient CO₂ fixation, high oil content and ease of processing (no lignin in their
17 structure). Besides, they do not compete with productive lands (Azizi et al., 2017).
18

19 The heating value of microalgae bio-oil is relatively high, usually in the 27-42 MJ/kg range,
20 which is remarkably higher than those for the bio-oils derived from lignocellulosic biomass
21 (Yang et al., 2019). Furthermore, the carbon and hydrogen contents of the bio-oils obtained from
22 microalgae pyrolysis are in the 51-82 and 7-12 % ranges, respectively, depending on pyrolysis
23 conditions and microalgae nature (Yang et al., 2019), whereas those corresponding to fossil fuels
24 are usually in the 83-87% and 10-14% ranges, respectively. Interestingly, sulfur content of
25 microalgae bio-oil is also low. It should be noted that microalgae contain lipids, proteins and
26 carbohydrates, whereas lignocellulosic biomass is mainly made up of cellulose, hemicellulose
27 and lignin (Gautam and Vinu, 2018; Suganya et al., 2016).
28

29 Solid, liquid or gaseous bio-fuels may be obtained from microalgae via two different pathways,
30 i.e., biochemical and thermochemical processes. In the biochemical processes, microorganisms
31 are used to convert the biomass into bio-fuels. In the thermochemical process, biomass is heated
32 under inert or reactive atmosphere and converted into solid, liquid and gaseous bio-fuels.
33
34
35
36
37
38
39
40
41
42
43
44
45
46
47
48
49
50
51
52
53
54
55
56
57
58
59
60
61
62
63
64
65

1
2
3
4 However, biomass conversion through thermochemical processes is more favorable due to the
5
6 low conversion, high production cost and lengthy reaction steps of the biochemical methods
7
8
9 (Raheem et al., 2015).

10
11 The thermochemical routes for the conversion of biomass may be categorized into combustion,
12
13 gasification, liquefaction and pyrolysis (W. H. Chen et al., 2018). Of all thermochemical
14
15 conversion processes, pyrolysis (thermal degradation of matter in the absence of oxygen) at a
16
17 temperature ranging from 400 to 600 °C followed by direct condensation of vapors is a promising
18
19 and cost effective method, which plays a crucial role in biomass conversion (Yildiz et al., 2014).
20
21
22
23 Microalgae pyrolysis performance is greatly influenced by process conditions, especially,
24
25 heating rate, temperature and residence time (Azizi et al., 2017). Accordingly, reactor design
26
27 plays a key role in product distribution and their composition. A wide variety of reactor designs
28
29 have been proposed in the literature, as are slow (fixed beds or autoclave reactors) and fast
30
31 pyrolysis reactors (fluidized and free fall reactors) (Li et al., 2019). Pyrolysis of *Spirulina*
32
33 *plantensis* in a fixed bed reactor showed that temperature in the 400-700°C range influenced
34
35 products yields. The highest bio-oil, bio-gas and bio-char yields were obtained at 500, 700 and
36
37 400 °C, respectively. Higher temperatures decreased bio-oil production and increased bio-gas
38
39 production (Jafarian and Tavasoli, 2018). Pyrolysis of microalgae *Chlorella protothecoides* and
40
41 *Microcystis aeruginosa* in a fluidized bed reactor led to higher saturated and polar fractions of
42
43 microalgae bio-oil than those in the bio-oil from wood. Besides, distribution of straight-chain
44
45 alkanes in the saturated fractions of microalgae bio-oil were similar to those in diesel fuel (Miao
46
47 et al., 2004). Pyrolysis of the lipid residue extracted from the microalgae *Tribonema minus* in a
48
49 fixed bed reactor showed that the major compounds in the bio-oil were carbonyls, hydrocarbons
50
51 and nitrogenous compounds, with a high content of oxygen in their structure. The main
52
53
54
55
56
57
58
59
60
61
62
63
64
65

1
2
3
4 components in the bio-gas were CO₂ and CO, and their contents changed with pyrolysis
5
6 temperature. Compared to lignocellulosic biomass, the liquid products of microalgae pyrolysis
7
8 contained more alkane/alkene and less aromatics (Ji et al., 2015). Pyrolysis of *Scenedesmus*
9
10 *dimorphus* in a fixed bed reactor showed that the bio-oil yield peaks at the temperature of 500 °C
11
12 and contains n-hexane, ethyl acetate, toluene and methanol (Bordoloi et al., 2015). Pyrolysis of
13
14 *Scenedesmus sp.* in a spouted-fluidized bed reactor produces bio-oil with an average calorific
15
16 value of 18.4 MJ/kg. Moreover, the total acid number of this bio-oil was lower than the standard
17
18 one produced from woody biomass (Harman-Ware et al., 2013). In summary, fixed beds and
19
20 fluidized beds reactors were commonly used to pyrolyse microalgae (Aboulkas et al., 2017;
21
22 Adamczyk and Sajdak, 2018). To our knowledge, pyrolysis of microalgae in a conical spouted
23
24 bed reactor has not been reported in previous literature.

25
26 Spouted bed reactors have been applied to study different thermochemical processes, as are
27
28 torrefaction, gasification, combustion and pyrolysis (Alvarez et al., 2018; Barbarias et al., 2018;
29
30 Wang et al., 2018). This type of reactor is suitable for handling different kinds of particles, from
31
32 coarse to fine materials, and even sticky solids, with no agglomeration and segregation problems
33
34 due to the vigorous solid circulation regime attained (Elordi et al., 2011). Moreover, the particle
35
36 movement in spouted bed reactors leads to higher heat transfer rates between particles and
37
38 phases (P K Mollick et al., 2019; Yaman et al., 2019), which makes them especially suitable for
39
40 the thermochemical conversion of biomass and waste (Perkins et al., 2018). In this study, a
41
42 conical spouted bed reactor was used for the pyrolysis of different microalgae species. Due to the
43
44 especial features of microalgae, specifically their low density and tendency to form fines,
45
46 insertion of a fountain confiner in the conical spouted bed was considered to avoid the elutriation
47
48 of non-reacted microalgae fine particles (Altzibar et al., 2017). In addition, this device greatly
49
50
51
52
53
54
55
56
57
58
59
60
61
62
63
64
65

1
2
3
4 improves the hydrodynamic performance of the reactor, as it enhances the gas-solid contact in
5
6 the fountain region and leads to a highly stable bed. It is to note that a remarkable improvement
7
8 in conversion efficiency was reported when biomass steam gasification was conducted in the
9
10 mentioned bed provided with fountain confiner (Cortazar et al., 2018).
11
12

13
14 The aim of this study is to delve into the pyrolysis of the microalgae *Nannochloropsis*,
15
16 *Tetraselmis* and *Isochrysis galbana* in a conical spouted bed reactor. The experiments were
17
18 carried out at the temperature of 500 °C. Product yields (bio-oil, bio-gas and bio-char) were
19
20 determined and compared with those obtained in other types of reactors. Besides, the pyrolytic
21
22 products were characterized based on GC and GC-MS and on ultimate and proximate analyses.
23
24 Finally, a reaction scheme was proposed based on the bio-oil composition obtained from GC/MS
25
26 analysis.
27
28
29

30 31 **2. Material and methods**

32 33 **2.1. Feedstock characterization**

34
35 Three freeze-dried microalgae *Nannochloropsis (NC)*, *Tetraselmis (TS)* and *Isochrysis galbana*
36
37 (*IG*) have been used as feedstock. The microalgae were produced at the University of Almeria,
38
39 Spain. Briefly, they were cultivated in tubular photo-bioreactors operating in continuous mode,
40
41 with the feed being seawater containing nutrient source. The ultimate and proximate analysis
42
43 were carried out in a CHN elemental analyzer (LECO CHNS-932) and in a thermobalance (TGA
44
45 Q500IR), respectively. The higher heating value (HHV) was measured according to the method
46
47 described elsewhere (Azizi et al., 2018). The results are shown in Table 1.
48
49
50
51

52 53 **Table 1**

54
55 The pyrolysis behavior of the different microalgae samples has been studied in a TGA Q500IR
56
57 thermobalance. The experiments were carried out with a heating rate of 15 °C min⁻¹ and with a
58
59
60
61

1
2
3
4 nitrogen flow rate of 100 ml min⁻¹. As observed in Figure 1, the three evaluated microalgae
5
6 showed a similar degradation pattern, i.e., pyrolysis was completed when temperature reached
7
8 500-550 °C and the maximum weight loss rate occurs between 295 and 320 °C. Microalgae
9
10 pyrolysis starts with moisture evaporation at around 100 °C, and the main degradation occurs
11
12 between 200 and 600 °C. In this stage, all components (carbohydrates, proteins, lipids, and other
13
14 minor ones) are pyrolysed (Bach and Chen, 2017). It should be noted that the degradation of
15
16 carbohydrates and proteins overlap (main peak) (Chen et al., 2014), whereas the degradation of
17
18 lipids appears at higher temperatures and may be associated with the shoulder in the 400-500 °C
19
20 range (López-González et al., 2015).
21
22
23
24
25

26 Figure 1

27 28 **2.2. Pyrolysis plant**

29
30
31 Pyrolysis of microalgae was carried out in a bench scale unit with a conical spouted bed reactor
32
33 made of stainless steel. The development of this reaction unit is based on the wide experience
34
35 gained in the pyrolysis of different solid wastes, such as tires, plastics and different biomasses
36
37 (Elordi et al., 2011). The performance of this reactor has been improved with the insertion of a
38
39 draft tube and a fountain confiner. The draft tube improves the stability of the spouting regime,
40
41 controls the solid circulation rate and reduces the gas flow rate required for operation (Palash
42
43 Kumar Mollick et al., 2019). The fountain confiner is crucial for handling fine and low density
44
45 materials, as it avoids their elutriation prior to full conversion, apart from contributing to bed
46
47 stability (Altzibar et al., 2017).
48
49
50
51

52
53 The detailed design of this reactor provided with draft tube and fountain confiner is shown in
54
55 Figure 2. These dimensions were established based in the knowledge acquired in the previous
56
57 hydrodynamic studies (Altzibar et al., 2017). Thus, the gas inlet diameter is 1 cm and that of the
58
59
60
61
62
63
64
65

1
2
3
4 bottom 2 cm. The total height and that of conical section are 34 cm and 20.5 cm, respectively.
5
6
7 The angle of the conical section is 28° ($\gamma/2$). The draft tube diameter 1 cm and the height of
8
9 entrainment zone 2.5 cm. Finally, a fountain confiner with a diameter of 8 cm was welded to the
10
11 reactor lid, with the total length of this device being 8.2 cm.
12

13 14 **Figure 2**

15
16 The reactor was heated with an electric oven and temperature was monitored with a
17
18 thermocouple located in the sand bed. Downstream the reactor, a high-efficiency cyclone and a
19
20 sintered steel filter retain the fines dragged by the gaseous stream. Both devices are located in a
21
22 convection oven maintained at 300°C to avoid the condensation of bio-oil prior to condensation.
23
24 The condensation system is made up of a double-shell tube condenser cooled by tap water and a
25
26 steel filter. Finally, the gases leaving the condensation system were filtered by coalescence filters
27
28 in order to remove bio-oil droplets prior to their analysis in a micro-gas chromatograph (micro-
29
30 GC). The plant has an original piston feeding system that allows for continuous microalgae
31
32 feeding without operational problems. Further details about the pyrolysis unit are reported
33
34 elsewhere (Alvarez et al., 2018).
35
36
37
38
39
40

41 **2.3. Experimental procedure**

42
43 The pyrolysis experiments were carried out in continuous mode by feeding 1 g min^{-1} of
44
45 microalgae. A bed of 150 g of sand with a particle size of 100-150 μm was used to ensure high
46
47 heat transfer rates inside the reactor, and therefore operation under isothermal conditions. The
48
49 nitrogen flow rate was set at 1.5 times the minimum for spouting (3.5 l min^{-1}) to ensure stable
50
51 spouting and short residence times of the volatiles generated in the reactor. The pyrolysis
52
53 experiments were carried out 500°C , which, as observed in Figure 1, is the minimum
54
55 temperature for full conversion of microalgae into volatiles. In addition, operating at 500°C bio-
56
57
58
59
60
61
62
63
64
65

1
2
3
4 oil cracking reactions to produce gaseous products can be attenuated ensuring a high production.
5
6 In fact this temperature has been usually regarded as the optimum one for bio-oil production
7
8 from microalgae (Azizi et al., 2018) and more specifically, in the pyrolysis of different
9
10 biomasses in conical spouted bed reactors (Alvarez et al., 2018; Amutio et al., 2012). When the
11
12 reactor was heated to the desired temperature, the microalgae were continuously fed into the
13
14 reactor by the piston feeder. Samples were heated rapidly and the volatiles entrained from the
15
16 reactor by using nitrogen as carrier gas. The condensable volatiles were trapped in the condenser,
17
18 which was cooled by tap water, and then passed through the filter to trap the volatiles as much as
19
20 possible. The non-condensable gas was analyzed in the gas chromatograph and then vented to
21
22 the atmosphere. After each experiment, the reactor was cooled to the ambient temperature with
23
24 nitrogen and the char was collected for subsequent analysis.
25
26
27
28
29

30 31 **2.4. Product characterization**

32
33 The volatile stream leaving the reactor was analyzed on-line in a gas chromatograph (Varian
34
35 3900) equipped with a flame ionization detector (FID). The outlet of the reactor to the
36
37 chromatograph was heated to a temperature of 280 °C to avoid condensation of heavy bio-oil
38
39 compounds. In order to determine correctly the gas and bio-oil yields based on the analysis in the
40
41 gas chromatograph, cyclohexane was used as external reference because it is not formed in the
42
43 process. Given that microalgae pyrolysis was carried out in continuous regime, the gaseous
44
45 product yields may be assessed by comparing their concentration with that of cyclohexane. Thus,
46
47 a constant flow rate of 0.05 ml min⁻¹ was injected into the reactor and analyzed in the GC
48
49 together with the volatile products formed. Non-condensable gaseous products were analyzed in
50
51 a micro chromatograph (Varian 4900). It was equipped with three independent analytical
52
53 modules, namely, Molecular sieve 5, Porapak (PPQ) and Plot Alumina. It is worth noting that all
54
55
56
57
58
59
60
61
62
63
64
65

1
2
3
4 the runs were repeated at least 3 times under the same experimental conditions to guarantee
5
6 reproducibility of the results.
7

8
9 The lower heating value (LHV) of the gaseous products was determined according to following
10
11 equation (Chen et al., 2017a);
12

$$13 \quad LHV \left(MJ/m^3 \right) = 0.126CO + 0.108H_2 + 0.358CH_4 + 0.665C_nH_m \quad (Eq. 1)$$

14
15
16
17

18 where CO, H₂ and CH₄ are the volume fractions of carbon monoxide, hydrogen and methane in
19
20 the gaseous stream, respectively. C_nH_m corresponds to any other light hydrocarbon in the gas.
21
22

23 The main components of the bio-oil were identified by gas chromatography-mass spectroscopy
24
25 (Shimadzu QP-2010S). The surface characteristics of the chars were obtained by using a
26
27 Scanning Electronic Microscope (JEOL JSM-6400). The ultimate, proximate and HHV of the
28
29 char were determined by the method explained before.
30
31

32 33 **3. Results and discussion**

34 35 **3.1. Product yields**

36
37 The main products obtained in the pyrolysis may be categorized into gas, liquid and solid. The
38
39 product yields obtained in the pyrolysis of different microalgae species are shown in Figure 3. As
40
41 expected, bio-oil is the main product obtained in the fast pyrolysis of the three microalgae
42
43 species. The pyrolysis product distribution obtained with *NC* is similar to that obtained with *TS*,
44
45 with bio-oil, bio-gas and bio-char yields being 58%, 13% and 30%, respectively. *IG* showed a
46
47 different pyrolysis behavior, with bio-oil yield being the highest (66%) and bio-char yield the
48
49 lowest (21%). However, the gas yield in the pyrolysis of *IG* is similar to the other two
50
51 microalgae. The higher and lower yields of bio-oil and bio-char obtained from the pyrolysis of
52
53 *IG* may be conditioned by its higher volatile content compared to *NC* and *TS* which clearly
54
55 evidences the higher potential for bio-oil production of *IG*.
56
57
58
59
60
61
62
63
64
65

1
2
3
4 In order to evaluate the performance of the conical spouted bed reactor, the bio-oil yields of
5
6 microalgae have been compared with those obtained in the pyrolysis of microalgae in different
7
8 reactor configurations. However, direct comparison is really challenging, as product distribution
9
10 strongly depends on pyrolysis conditions, reactor design and microalgae characteristics (Li et al.,
11
12 2019). On the one hand, in the slow pyrolysis of microalgae, the sample is heated slowly and the
13
14 residence time is high (even minutes), which promote the production of a high solid fraction. On
15
16 the other hand, fast pyrolysis of microalgae leads mainly towards the production of bio-oil (Yang
17
18 et al., 2019). It should be noted that the bio-oil yields obtained in this study in the pyrolysis of
19
20 different microalgae are in general higher than those reported in the literature in different
21
22 technologies, such as fixed reactors, screw kilns, microwave ovens and even fluidized beds
23
24 (Aboulkas et al., 2017; Du et al., 2011; Miao et al., 2004; Sotoudehniakarani et al., 2019; Yang
25
26 et al., 2019). Thus, Yuan et al. (Yuan et al., 2015) obtained the highest bio-oil yield of 32.69
27
28 wt% from *Chlorella vulgaris* pyrolysis in a fixed bed reactor operating at 500 °C. Bio-oil
29
30 production from microalgae *Scenedesmus sp.* in a fluidized bed reactor at 440 °C was of around
31
32 52 wt% (Kim et al., 2014). Likewise, the pyrolysis of *Chlorella vulgaris* in a fluidized bed
33
34 reactor at 500 °C led to a total bio-oil yield of around 53 wt% (Wang et al., 2013).

35
36 The cyclic movement of the particles in the conical spouted bed reactor promotes thermal
37
38 distribution inside the bed and fast heating rates. Besides, the gas residence time in the bed is
39
40 particularly low. The aforementioned features reduce secondary reactions in the gas phase, which
41
42 decrease by-product formation and improve bio-oil production. Although, especially high bio-oil
43
44 yields are obtained in this study involving microalgae pyrolysis in a conical spouted bed reactor,
45
46 these values are still lower than those obtained in lignocellulosic biomass pyrolysis in the same
47
48 type of reactor (Amutio et al., 2015, 2012). This fact is due to the different nature of
49
50
51
52
53
54
55
56
57
58
59
60
61
62
63
64
65

1
2
3
4 lignocellulosic biomass, with higher volatile matter and lower ash content. The water content in
5
6 the bio-oil is a fact of high relevance for its subsequent use. Thus, the bio-oils from *NC*, *IG* and
7
8 *TS* contain 26.79%, 24.81% and 24.33%, respectively. The lower water content of microalgae
9
10 compared to lignocellulosic biomass is probably due to the lower oxygen content of microalgae
11
12 (W. H. Chen et al., 2018). This is an interesting feature for the downstream utilization of bio-oil,
13
14 as it leads to higher heating value and lower acid corrosion of equipment. The bio-char yield was
15
16 20-30 wt%, which is higher than those obtained from lignocellulosic biomasses, and is explained
17
18 by the higher ash and fixed carbon contents of microalgae. The gas yield is of around 12 wt% for
19
20 all the studied microalgae, which is lower than those reported in the literature in different
21
22 pyrolysis technologies at similar temperatures (Aboulkas et al., 2017; Beneroso et al., 2013; Du
23
24 et al., 2011; Sotoudehniakarani et al., 2019). Moreover, the gas yields produced from microalgae
25
26 pyrolysis are comparable to those obtained from lignocellulosic biomasses (of around 10 wt%) in
27
28 the spouted bed reactor, which remarks the capacity of this reactor for avoiding bio-oil cracking
29
30 reactions (Amutio et al., 2012). It is to note that this technology was successfully scaled up for
31
32 biomass pyrolysis. Therefore, a pilot plant with a capacity of 25 kg h⁻¹ of biomass continuous
33
34 feed rate was developed (Fernandez-Akarregi et al., 2013). Thus, the suitable results obtained in
35
36 bench scale units (Amutio et al., 2012) were confirmed in the pilot plant unit. The promising
37
38 performance showed by conical spouted bed reactor in microalgae pyrolysis with higher bio-oil
39
40 yields than other technologies and the reported scalability of this technology clearly remark the
41
42 industrial relevance of the present results.
43
44
45
46
47
48
49
50
51

52
53 **Figure 3**
54

55 **3.2. Bio-gas characterization**

56
57
58
59
60
61

1
2
3
4 The non-condensable gaseous stream is made up of mainly hydrogen, carbon monoxide and
5
6 carbon dioxide with their concentrations being 10-19 vol%, 10-19 vol% and 50-65 vol%,
7
8 respectively. Other light hydrocarbons, such as methane, ethane, ethylene, propane and
9
10 propylene, were also detected. Methane is the prevailing light hydrocarbon, whose concentration
11
12 is the highest (10 vol%) in the pyrolysis of *TS*. These results are consistent with the gas
13
14 compositions reported in the literature for microalgae pyrolysis under mild conditions (Beneroso
15
16 et al., 2013; Du et al., 2011; Maliutina et al., 2017).
17
18
19
20

21 Microalgae main components are lipids, proteins and carbohydrates. Carbon dioxide is the main
22
23 gaseous product, which is mainly produced from the cracking of carbonyl and carboxyl groups in
24
25 carbohydrates and proteins (Chen et al., 2017b). Carbon monoxide is formed in the cracking of
26
27 ether bonds and carbonyl groups. The formation of hydrogen is related to radical
28
29 polycondensation from microalgae volatiles. The formation of methane should be attributed to
30
31 the demethoxylation of algae. The other gaseous products are formed by scission and cyclization
32
33 reactions of long chain fatty acids in the microalgae (Chen et al., 2017b).
34
35
36
37

38 The LHV of the gaseous streams was also determined, with their values being 11.6, 11.64 and
39
40 9.45 MJ/m³ for *NC*, *IG* and *TS*, respectively. These heating values are conditioned by the high
41
42 CO₂ content, higher than 50 % vol. for all the microalgae studied. It is to note that the quality of
43
44 these gases may be greatly improved operating at higher temperatures, as they allow increasing
45
46 H₂ and CH₄ yields and decreasing those of CO and CO₂ (Maddi et al., 2011). The gaseous stream
47
48 may be used not only as power or heat supplier, but also as feedstock for chemical process, such
49
50 as Fischer-Tropsch synthesis subsequent to an upgrading process.
51
52
53
54

55 **Figure 4**

56 **3.3. Bio-oil characterization**

57
58
59
60
61
62
63
64
65

1
2
3
4 The concentrations determined by GC/MS analysis for the bio-oil compounds were obtained
5
6 from the pyrolysis of microalgae species. The identified compounds contain a wide range of
7
8 organic compounds, and they have been categorized into hydrocarbons (saturated, unsaturated
9
10 and aromatic hydrocarbons), nitrogenous compounds (NCC) (nitrile, amine, amide, azole, indole
11
12 and nitrogen heterocyclic compounds (NHC)), ketones, alcohols, acids, lactones, phenols and
13
14 aldehydes. Figure 5 shows the yields of the families of chemical compounds in the bio-oils
15
16 derived from the three microalgae. It should be noted that many other compounds not belonging
17
18 to the mentioned groups have also been obtained, but they have low match factors in the GC/MS.
19
20 The mass balance has been closed based on the areas of the chromatographic signals (Gautam
21
22 and Vinu, 2018).
23
24
25
26
27

28 Figure 5

29
30 The main compounds produced in the pyrolysis of *NC* were ketones, NCC and hydrocarbons,
31
32 with their yields being 13.57 %wt, 11.02 %wt and 11.02 %wt, respectively. The yield of alcohols
33
34 produced in the the pyrolysis of *NC* is 4.97 %wt. Regarding *TS*, NCC (16.91 %wt),
35
36 hydrocarbons (16.23 %wt) and alcohols (11.9 %wt) are the main components in the bio-oil.
37
38 Ketones are also produced in the the pyrolysis of *TS* and their yield is 4.16 %wt. In the case of
39
40 *IG*, alcohols (28.38 %wt), hydrocarbons (21.12 %wt) and NCC (8.45 %wt) are the main
41
42 components. Ketones are also produced and their yield is 1.67 %wt. Although the yields of other
43
44 compounds are rather low, some of them are of interest from the perspective of their specific
45
46 applications. Thus, a low yield of lactones is present in the pyrolysis of *NC* and *TS* green
47
48 microalgae.
49
50
51
52
53

54
55 The compounds obtained in the bio-oil are related to the chemical composition of the original
56
57 microalgae, i.e., to the relative content of lipids, proteins and carbohydrates. Thus, NCC are
58
59
60
61
62
63
64
65

1
2
3
4 formed by the decomposition of proteins in microalgae, whose structure varies in a wide range
5 depending on the species. Thus, *NC* and *TS* are green microalgae, whereas *IG* is a kind of brown
6 microalga. The content of hydrocarbons in the liquid product is an index of the potential of the
7 biomass as a raw material to produce bio-fuels and bio-components (Adamczyk and Sajdak,
8 2018), and they are mainly produced by the cracking of lipids. Oxygen is in the bio-oil mainly
9 within oxygen containing organic compounds (acids, ketones, aldehydes, alcohols, furans,
10 phenols, lactones) (Yuan et al., 2015). The formation of most oxygenated compounds is
11 attributed to the thermal decomposition of carbohydrates and lipids in algal biomass (Bordoloi et
12 al., 2015), but phenolic compounds stem from protein thermal decomposition (Maliutina et al.,
13 2017). At temperatures higher than 400°C, carbonyl groups have low thermal stability and
14 undergo decarbonylation reactions leading to ketones, aldehydes and carbon dioxide (Chen et al.,
15 2017b). The presence of oxygen compounds, such as acids, ketones and aldehydes in the bio-oil
16 is responsible for its instability and corrosiveness during transport and storage. Furthermore, the
17 presence of ethers and esters in the bio-oil reduces its heating value (Zainan et al., 2018).

3.4. Bio-char characterization

18
19 The ultimate analysis of the bio-chars obtained from the pyrolysis of algal biomass at 500 °C is
20 shown in Table 2. As observed, the oxygen and hydrogen contents of the bio-char are lower than
21 those of the raw microalgae. This reduction in hydrogen and oxygen content is due to
22 aromatization, decarbonylation, dehydration and decarboxylation reactions (Aboulkas et al.,
23 2017). The nitrogen content of microalgae bio-char is significantly higher than those of other
24 bio-chars (Alvarez et al., 2019, 2018), and is explained by the protein content of microalgae.
25 Furthermore, the higher nitrogen content of this bio-char increases its value as soil amender, but
26 its high ash content is a disadvantage for this application (Sotoudehniakarani et al., 2019). The

1
2
3
4 carbon content of algal bio-char is relatively high, making it suitable as a renewable solid fuel
5
6
7 (Aboulkas et al., 2017).
8

9 **Table 2**

10
11 The morphology of raw microalgae and their bio-chars has been studied by using scanning
12
13 electron microscopy (SEM). There are significant differences between the morphologies of the
14
15 microalgae and their chars. As observed, the parent biomasses have a relatively smooth surface
16
17 compared to those of the chars, whose surface is full of holes created during the pyrolysis
18
19 process due to the release of volatile compounds. As a result, the porosity, and so the surface
20
21 area, of the parent biomasses is lower than those of the bio-chars. Thus, pyrolysis improves the
22
23 morphology and porous structure of raw material.
24
25
26
27

28 **3.5. Possible pyrolysis pathways in the fast pyrolysis of microalgae**

29
30 Microalgae main components have different pyrolysis pathways, which explains their selective
31
32 formation. Triglycerides are the main components of lipids. Carbohydrate is a component
33
34 containing carbon, hydrogen and oxygen atoms, which are connected to each other to form
35
36 different structures. *It is to note that the carbohydrates present in the microalgae are in the form*
37
38 *of polysaccharides and oligosaccharides (Yang et al., 2019).* Although proteins have complex
39
40 structures and each microalga species has different types of proteins, their basic units are amino
41
42 acids, which are connected by peptide bonds. Each amino acid contains amine and carboxyl
43
44 functional groups along with a side chain, which is specific to each amino acid. Possible
45
46 pyrolysis pathways responsible for the thermal decomposition of microalgae components during
47
48 pyrolysis have been proposed.
49
50
51
52
53

54
55 *During pyrolysis, the acyl chains of triglycerides are separated from the glycerol backbone*
56
57 *through hydrolyze or cracking process. Such processes result in long chain fatty acids*
58
59
60
61

1
2
3
4 production. Fatty acids can go further through more reactions including decarboxylation,
5
6 decarbonylation, fragmentation of glycerin and C-C bond cleavage to form hydrocarbons, acids,
7
8 esters, alcohols and C₁-C₃ gases (Gautam and Vinu, 2018; Yang et al., 2019). It should be
9
10 mentioned that although hydrocarbons production is due to pyrolysis of carbohydrate, lipid and
11
12 protein, production of aliphatic hydrocarbons are mainly attributed to the cracking of lipids.
13

14
15 The reactions occurring during the pyrolysis of proteins are deamination, dehydration,
16
17 decarboxylation, cyclization and deoxygenation to form nitrogen containing compounds, such as
18
19 nitriles, amines, amides, hydrocarbons and nitrogen-heterocyclic compounds (Qi et al., 2018). It
20
21 should be mentioned that the generation of aromatic hydrocarbons is associated with the
22
23 presence of aromatic amino acids in the microalgae protein (Wang et al., 2013). Thus, the
24
25 thermal degradation of amino acid chains give way to the formation of different aromatics such
26
27 as toluene, xylene, and phenols, moreover and nitrogen containing heterocyclic compounds such
28
29 as indoles are also formed. Furthermore, the formation of olefins could also occur via cracking,
30
31 deoxygenation, and deamination reactions of protein degradation intermediates (Yang et al.,
32
33 2019).
34
35

36
37 Carbohydrate pyrolysis produces oxygen-containing compounds and water, which is the major
38
39 pyrolysis product (Wang et al., 2017). Primary reactions during pyrolysis of carbohydrates are
40
41 dehydration, bond cleavage, ring scission, deoxygenation and rearrangement to form cyclic
42
43 ketones, acids, aldehydes and other hydrocarbons (Yu et al., 2018). For instance, carbohydrates
44
45 are converted into furans and olefins through dehydration and deoxygenation reactions (Chen et
46
47 al., 2017b; Qi et al., 2018). Cyclization reactions and Diels–Alder condensation reactions convert
48
49 olefins into aromatics. It should be pointed out that the extent of the reaction strongly depends on
50
51
52
53
54
55
56
57
58
59
60
61
62
63
64
65

1
2
3
4 reaction conditions. Thus, these reaction mechanisms are favored by high temperatures and
5
6 residence times of pyrolysis volatiles.
7

8
9 Interactions can also occur between microalgae components during pyrolysis. One of these
10
11 interactions is Maillard reaction, which occurs between the intermediates from carbohydrate and
12
13 protein pyrolysis. These interactions lead to a large number of products such as heterocyclic
14
15 compounds containing nitrogen and oxygen, ultra violet absorbing intermediate and dark brown
16
17 polymeric compounds (Wang et al., 2017). Amino acids and fatty acid react with each other to
18
19 form protein-fatty acid surfactants and detergents. Lipophilic and hydrophilic group of surfactant
20
21 are from fatty acid (lipid) and amino acid (protein), respectively. Interactions between
22
23 carbohydrates and lipids produce alkyl polyglycoside surfactants (Wang et al., 2017). The
24
25 hydrophilic group is from carbohydrate and the lipophilic group is from lipid. However, almost
26
27 no biosurfactant nor detergent has been detected in the final bio-oil, which may be due to the
28
29 high pyrolysis temperature. Biosurfactant such as alkyl polyglycoside can be produced at lower
30
31 pyrolysis temperatures.
32
33
34
35
36
37

38 It should be noted that oxygen rich compounds of the microalgae are decomposed during the
39
40 pyrolysis and oxygen is removed as CO, CO₂ and H₂O (Yu et al., 2018). Cracking and steam
41
42 reforming of lipids release CO₂, CO, H₂ and CH₄ through decarboxylation, decarbonylation,
43
44 dehydrogenation and demethylation (Chen et al., 2017b)
45
46
47

48 **3.6. Applications of bio-char, bio-oil and bio-gas**

49

50 The bio-char has various potential applications, as are those related to solid fuel for bio-energy,
51
52 carbon sequestration agent, soil amender and absorbent for removal of heavy metals from waste
53
54 water or pollutants from gaseous streams (Maliutina et al., 2017). The heating value of the
55
56 gaseous stream is moderate, and may therefore be used for power generation or heat supplying.
57
58
59
60
61
62
63
64
65

1
2
3
4 Besides, hydrogen and carbon monoxide may be used as feedstock to synthesize hydrocarbons
5
6 through Fischer-Tropsch process (Chen et al., 2017b). Bio-oil has been considered a promising
7
8 bio-fuel for generating heat, power and combined heat-power, but it may also be used as an
9
10 intermediate feedstock for the production of chemicals. The major constituents of bio-oil are
11
12 hydrocarbons, NCC, phenols, alcohols, acids, ketones and other oxygenated compounds. Among
13
14 these compounds, hydrocarbons are valuable components to be used as fuel. More specifically,
15
16 aromatic hydrocarbons may be used as an additive to increase the octane number of industrial
17
18 chemicals and transport fuels (Bordoloi et al., 2015). Although great efforts have been made for
19
20 the removal of oxygen and nitrogen containing compounds from the bio-oil (Li et al., 2019),
21
22 some of them may be a source of valuable chemicals. Thus, NCCs have a great potential for use
23
24 as platform chemicals in pharmaceutical and polymer industries (Carbas et al., 2017). Some
25
26 phenols and phenol derivatives can be used as food antioxidant, transportation fuel additives,
27
28 precursors for chemical products and in resin industry (Negahdar et al., 2016). Oxygenated
29
30 compounds lead to high corrosiveness, instability and low energy density. Therefore, their
31
32 content in the bio-oil must be decreased by using catalysts (W. Chen et al., 2018). Moreover,
33
34 several bio-oil upgrading routes have been proposed in the literature for the production of
35
36 commercial fuels, the following ones are those with better perspectives for their implantation: i)
37
38 Catalytic cracking, the use of acid catalysts as zeolites allows for the deoxygenation of bio-oil
39
40 with the subsequent production of hydrocarbons, usually of olefinic and aromatic nature. ii)
41
42 Catalytic hydrodeoxygenation /hydrocracking, this strategy is performed under hydrogen
43
44 pressures and using metallic catalysts. The use hydrogen allows for the production of
45
46 hydrocarbons from bio-oil, however the high external hydrogen demand of this process
47
48 represents a major challenge. iii) Electrocatalytic hydrogenation, this novel strategy pursues
49
50
51
52
53
54
55
56
57
58
59
60
61
62
63
64
65

1
2
3
4 stabilization and upgrading of bio-oil to form chemicals and fuels. This process is performed in
5
6 the presence of catalyst and under milder conditions in relation to conventional
7
8 hydrodeoxygenation. iv) Catalytic steam reforming, this process is performed at relatively high
9
10 temperatures (>600 °C) and steam/bio-oil ratios, the use of metallic catalysts (Ni based are the
11
12 most common ones) allow for high hydrogen productions. It should be noted that both catalytic
13
14 cracking and hydrocracking can be performed in refinery units by co-feeding bio-oil mixed with
15
16 conventional refinery streams. This possibility reinforces the interest of these alternatives as long
17
18 as already existing units can be used for bio-oil upgrading. Moreover, other less ambitious and
19
20 simple alternatives for bio-oil pretreatment after an utilization as low grade fuel are esterification
21
22 and emulsification.
23
24
25
26
27

28 **5. Conclusions**

29
30 Bio-oil was the main product obtained through pyrolysis of three microalgae species. The higher
31
32 bio-oil yield of *IG* is due to its higher volatile content compared to *NC* and *TS*. Heating value of
33
34 gaseous products shows that bio-gas may be used as power or heat supplier. Bio-oil constituents
35
36 were categorized into hydrocarbons, NCC and oxygenated compounds. Formation of NCC may
37
38 be attributed to the decomposition of protein in microalgae. Hydrocarbons mainly came from the
39
40 cracking of lipids during the pyrolysis of microalgae. The formation of oxygenated compounds is
41
42 attributed to the thermal decomposition of carbohydrates and lipids in algal biomass.
43
44
45
46
47

48 **Supplementary data**

49
50 E-supplementary data for this work can be found in e-version of this paper online
51

52 **Acknowledgment**

53
54 Kolsoom Azizi is grateful for the financial support from the Ministry of Science, Research and
55
56 Technology, Tehran, Iran. Kolsoom Azizi and Mostafa Keshavarz Moraveji thank the
57
58
59
60
61

1
2
3
4 Department of Chemical Engineering, University of Basque Country UPV/EHU, for the
5
6 technical support. This work was carried out with financial support from the Spain's Ministries
7
8 of Economy and Competitiveness (CTQ2016-75535-R (AEI/FEDER, UE)) and Science,
9
10 Innovation and Universities (RTI2018-098283-J-I00 (MINECO/FEDER, UE)), the Basque
11
12 Government (IT1218-19), and the European Union's Horizon 2020 research and innovation
13
14 programme under the Marie Skłodowska-Curie grant agreement No. 823745.
15
16
17

18 **References**

- 21 [1] Aboulkas, A., Hammani, H., Achaby, M. El, Bilal, E., Barakat, A., El, K., 2017. Valorization
22
23 of algal waste via pyrolysis in a fixed-bed reactor : Production and characterization of bio-
24
25 oil and bio-char. *Bioresour. Technol.* 243, 400–408.
26
27 <https://doi.org/10.1016/j.biortech.2017.06.098>
28
29
30
31 [2] Adamczyk, M., Sajdak, M., 2018. Pyrolysis Behaviours of Microalgae *Nannochloropsis*
32
33 *gaditana*. *Waste and Biomass Valorization* 9, 2221–2235. [https://doi.org/10.1007/s12649-](https://doi.org/10.1007/s12649-017-9996-8)
34
35 [017-9996-8](https://doi.org/10.1007/s12649-017-9996-8)
36
37
38 [3] Altzibar, H., Estiati, I., Lopez, G., Saldarriaga, J.F., Aguado, R., Bilbao, J., Olazar, M., 2017.
39
40 Fountain con fi ned conical spouted beds 312, 334–346.
41
42 <https://doi.org/10.1016/j.powtec.2017.01.071>
43
44
45 [4] Alvarez, J., Amutio, M., Lopez, G., Santamaria, L., Bilbao, J., Olazar, M., 2019. Improving
46
47 bio-oil properties through the fast co-pyrolysis of lignocellulosic biomass and waste tyres.
48
49 *Waste Manag.* 85, 385–395. <https://doi.org/10.1016/j.wasman.2019.01.003>
50
51
52
53 [5] Alvarez, J., Hooshdaran, B., Cortazar, M., Amutio, M., Lopez, G., Freire, F.B.,
54
55 Haghshenasfard, M., Hossein, S., Olazar, M., 2018. Valorization of citrus wastes by fast
56
57 pyrolysis in a conical spouted bed reactor. *Fuel* 224, 111–120.
58
59
60
61
62
63
64
65

- 1
2
3
4 <https://doi.org/10.1016/j.fuel.2018.03.028>
5
6
7 [6] Amutio, M., Lopez, G., Alvarez, J., Olazar, M., Bilbao, J., 2015. Fast pyrolysis of eucalyptus
8
9 waste in a conical spouted bed reactor. *Bioresour. Technol.* 194, 225–232.
10
11 <https://doi.org/10.1016/j.biortech.2015.07.030>
12
13
14 [7] Amutio, M., Lopez, G., Artetxe, M., Elordi, G., Olazar, M., Bilbao, J., 2012. Influence of
15
16 temperature on biomass pyrolysis in a conical spouted bed reactor. *Resour. Conserv.*
17
18 *Recycl.* 59, 23–31. <https://doi.org/10.1016/j.resconrec.2011.04.002>
19
20
21 [8] Azizi, K., Keshavarz Moraveji, M., Abedini Najafabadi, H., 2018. Simultaneous pyrolysis of
22
23 microalgae *C. vulgaris*, wood and polymer: The effect of third component addition.
24
25 *Bioresour. Technol.* 247, 66–72. <https://doi.org/10.1016/j.biortech.2017.09.059>
26
27
28 [9] Azizi, K., Keshavarz Moraveji, M., Abedini Najafabadi, H., 2017. A review on bio-fuel
29
30 production from microalgal biomass by using pyrolysis method. *Renew. Sustain. Energy*
31
32 *Rev.* 82, 3046–3059. <https://doi.org/10.1016/j.rser.2017.10.033>
33
34
35 [10] Bach, Q., Chen, W., 2017. Bioresource Technology Pyrolysis characteristics and kinetics of
36
37 microalgae via thermogravimetric analysis (TGA): A state-of-the-art review. *Bioresour.*
38
39 *Technol.* 246, 88–100. <https://doi.org/10.1016/j.biortech.2017.06.087>
40
41
42 [11] Barbarias, I., Lopez, G., Artetxe, M., Arregi, A., Bilbao, J., Olazar, M., 2018. Valorisation
43
44 of different waste plastics by pyrolysis and in-line catalytic steam reforming for hydrogen
45
46 production. *Energy Convers. Manag.* 156, 575–584.
47
48
49 <https://doi.org/10.1016/j.enconman.2017.11.048>
50
51
52 [12] Beneroso, D., Bermúdez, J.M., Arenillas, A., Menéndez, J.A., 2013. Microwave pyrolysis
53
54 of microalgae for high syngas production. *Bioresour. Technol.* 144, 240–246.
55
56
57 <https://doi.org/10.1016/j.biortech.2013.06.102>
58
59
60
61
62
63
64
65

- 1
2
3
4 [13] Bordoloi, N., Narzari, R., Sut, D., Saikia, R., Chutia, R.S., Kataki, R., 2015.
5
6 Characterization of bio-oil and its sub-fractions from pyrolysis of *Scenedesmus dimorphus*.
7
8 Renew. Energy 1–9. <https://doi.org/10.1016/j.renene.2016.03.081>
9
10
11 [14] Carbas, B.B., Kivrak, A., Kavak, E., 2017. Electrosynthesis of a new indole based donor-
12
13 acceptor-donor type polymer and investigation of its electrochromic properties. Mater.
14
15 Chem. Phys. 188, 68–74. <https://doi.org/10.1016/j.matchemphys.2016.12.040>
16
17
18 [15] Chen, W., Chen, Y., Yang, H., Xia, M., Li, K., Chen, X., Chen, H., 2017a. Co-pyrolysis of
19
20 lignocellulosic biomass and microalgae : Products characteristics and interaction effect
21
22 245, 860–868. <https://doi.org/10.1016/j.biortech.2017.09.022>
23
24
25 [16] Chen, W., Li, K., Xia, M., Yang, H., Chen, Y., Chen, X., Che, Q., Chen, H., 2018. Catalytic
26
27 deoxygenation co-pyrolysis of bamboo wastes and microalgae with biochar catalyst. Energy
28
29 157, 472–482. <https://doi.org/10.1016/j.energy.2018.05.149>
30
31
32 [17] Chen, W., Wu, Z., Chang, J., 2014. Isothermal and non-isothermal torrefaction
33
34 characteristics and kinetics of microalga *Scenedesmus obliquus* CNW-N. Bioresour.
35
36 Technol. 155, 245–251. <https://doi.org/10.1016/j.biortech.2013.12.116>
37
38
39 [18] Chen, W., Yang, H., Chen, Y., Xia, M., Yang, Z., Wang, X., Chen, H., 2017b. Algae
40
41 pyrolytic poly-generation: Influence of component difference and temperature on products
42
43 characteristics. Energy 131, 1–12. <https://doi.org/10.1016/j.energy.2017.05.019>
44
45
46 [19] Chen, W.H., Chu, Y.S., Liu, J.L., Chang, J.S., 2018. Thermal degradation of carbohydrates,
47
48 proteins and lipids in microalgae analyzed by evolutionary computation. Energy Convers.
49
50 Manag. 160, 209–219. <https://doi.org/10.1016/j.enconman.2018.01.036>
51
52
53 [20] Cortazar, M., Lopez, G., Alvarez, J., Amutio, M., Bilbao, J., Olazar, M., 2018. Advantages
54
55 of confining the fountain in a conical spouted bed reactor for biomass steam gasification.
56
57
58
59
60
61
62
63
64
65

- 1
2
3
4 Energy 153, 455–463. <https://doi.org/10.1016/j.energy.2018.04.067>
5
6
7 [21] Du, Z., Li, Y., Wang, X., Wan, Y., Chen, Q., Wang, C., Lin, X., Liu, Y., Chen, P., Ruan, R.,
8
9 2011. Microwave-assisted pyrolysis of microalgae for biofuel production. *Bioresour.*
10
11 *Technol.* 102, 4890–4896. <https://doi.org/10.1016/j.biortech.2011.01.055>
12
13
14 [22] Elordi, G., Olazar, M., Lopez, G., Artetxe, M., Bilbao, J., 2011. Continuous Polyolefin
15
16 Cracking on an HZSM-5 Zeolite Catalyst in a Conical Spouted Bed Reactor 6061–6070.
17
18
19 [23] Fernandez-Akarregi, A.R., Makibar, J., Lopez, G., Amutio, M., Olazar, M., 2013. Design
20
21 and operation of a conical spouted bed reactor pilot plant (25 kg/h) for biomass fast
22
23 pyrolysis. *Fuel Process. Technol.* 112, 48–56. <https://doi.org/10.1016/j.fuproc.2013.02.022>
24
25
26 [24] Gautam, R., Vinu, R., 2018. Non-catalytic fast pyrolysis and catalytic fast pyrolysis of
27
28 *Nannochloropsis oculata* using Co-Mo / γ -Al₂O₃ catalyst for valuable chemicals. *Algal*
29
30 *Res.* 34, 12–24. <https://doi.org/10.1016/j.algal.2018.06.024>
31
32
33 [25] Harman-Ware, A.E., Morgan, T., Wilson, M., Crocker, M., Zhang, J., Liu, K., Stork, J.,
34
35 Debolt, S., 2013. Microalgae as a renewable fuel source: Fast pyrolysis of *Scenedesmus*.
36
37 *Renew. Energy* 60, 625–632. <https://doi.org/10.1016/j.renene.2013.06.016>
38
39
40 [26] Jafarian, S., Tavasoli, A., 2018. A comparative study on the quality of bioproducts derived
41
42 from catalytic pyrolysis of green microalgae *Spirulina (Arthrospira) plantensis* over
43
44 transition metals supported on HMS-ZSM5 composite. *Int. J. Hydrogen Energy* 43, 19902–
45
46 19917. <https://doi.org/10.1016/j.ijhydene.2018.08.171>
47
48
49 [27] Ji, X., Liu, B., Chen, G., Ma, W., 2015. The pyrolysis of lipid-extracted residue of
50
51 *Tribonema minus* in a fixed-bed reactor. *J. Anal. Appl. Pyrolysis* 116, 231–236.
52
53 <https://doi.org/10.1016/j.jaap.2015.09.006>
54
55
56 [28] Kim, S.W., Koo, B.S., Lee, D.H., 2014. A comparative study of bio-oils from pyrolysis of
57
58
59
60
61
62
63
64
65

- 1
2
3
4 microalgae and oil seed waste in a fluidized bed. *Bioresour. Technol.* 162, 96–102.
5
6 <https://doi.org/10.1016/j.biortech.2014.03.136>
7
8
9 [29] Li, F., Srivatsa, S.C., Bhattacharya, S., 2019. A review on catalytic pyrolysis of microalgae
10 to high-quality bio-oil with low oxygenous and nitrogenous compounds. *Renew. Sustain.*
11 *Energy Rev.* 108, 481–497. <https://doi.org/10.1016/j.rser.2019.03.026>
12
13
14 [30] López-González, D., Puig-Gamero, M., Acién, F.G., García-Cuadra, F., Valverde, J.L.,
15 Sanchez-Silva, L., 2015. Energetic, economic and environmental assessment of the
16 pyrolysis and combustion of microalgae and their oils. *Renew. Sustain. Energy Rev.* 51,
17 1752–1770. <https://doi.org/10.1016/j.rser.2015.07.022>
18
19
20 [31] Maddi, B., Viamajala, S., Varanasi, S., 2011. Comparative study of pyrolysis of algal
21 biomass from natural lake blooms with lignocellulosic biomass. *Bioresour. Technol.* 102,
22 11018–11026. <https://doi.org/10.1016/j.biortech.2011.09.055>
23
24
25 [32] Maliutina, K., Tahmasebi, A., Yu, J., Saltykov, S.N., 2017. Comparative study on flash
26 pyrolysis characteristics of microalgal and lignocellulosic biomass in entrained-flow
27 reactor. *Energy Convers. Manag.* 151, 426–438.
28
29 <https://doi.org/10.1016/j.enconman.2017.09.013>
30
31
32 [33] Miao, X., Wu, Q., Yang, C., 2004. Fast pyrolysis of microalgae to produce renewable fuels.
33 *J. Anal. Appl. Pyrolysis* 71, 855–863. <https://doi.org/10.1016/j.jaap.2003.11.004>
34
35
36 [34] Mollick, P K, Goswami, P.S., Krishnan, M., Vijayan, P.K., Pandit, A.B., 2019. A novel
37 approach to correlate heat transfer and pressure fluctuation in gas – solid spouted bed.
38 *Particuology* 42, 26–34. <https://doi.org/10.1016/j.partic.2018.05.006>
39
40
41 [35] Mollick, Palash Kumar, Pandit, A.B., Vijayan, P.K., Krishnan, M., 2019. Critical
42 Assessment of Performance of a Draft Tube Configured in a Spouted Bed for Various
43
44
45
46
47
48
49
50
51
52
53
54
55
56
57
58
59
60
61
62
63
64
65

- 1
2
3
4 Fluid – Particle Properties. *Ind. Eng. Chem. Res.* 58, 19670–19680.
5
6 <https://doi.org/10.1021/acs.iecr.9b04032>
7
8
9 [36] Negahdar, L., Gonzalez-quiroya, A., Otyuskaya, D., Toraman, H.E., Liu, L., Jastrzebski,
10 J.T.B.H., Geem, K.M. Van, Marin, G.B., Thybaut, J.W., Weckhuysen, B.M., 2016.
11
12 Characterization and Comparison of Fast Pyrolysis Bio-oils from Pinewood, Rapeseed
13
14 Cake, and Wheat Straw Using ^{13}C NMR and Comprehensive GC \times GC 4974–4985.
15
16
17 <https://doi.org/10.1021/acssuschemeng.6b01329>
18
19
20
21 [37] Perkins, G., Bhaskar, T., Konarova, M., 2018. Process development status of fast pyrolysis
22
23 technologies for the manufacture of renewable transport fuels from biomass. *Renew.*
24
25 *Sustain. Energy Rev.* 90, 292–315. <https://doi.org/10.1016/j.rser.2018.03.048>
26
27
28 [38] Qi, P., Chang, G., Wang, H., Zhang, X., Guo, Q., 2018. Production of aromatic
29
30 hydrocarbons by catalytic co-pyrolysis of microalgae and polypropylene using HZSM-5. *J.*
31
32 *Anal. Appl. Pyrolysis* 136, 178–185. <https://doi.org/10.1016/j.jaap.2018.10.007>
33
34
35 [39] Raheem, A., Wan Azlina, W.A.K.G., Taufiq Yap, Y.H., Danquah, M.K., Harun, R., 2015.
36
37 Thermochemical conversion of microalgal biomass for biofuel production. *Renew. Sustain.*
38
39 *Energy Rev.* 49, 990–999. <https://doi.org/http://dx.doi.org/10.1016/j.rser.2015.04.186>
40
41
42 [40] Sotoudehniakarani, F., Alayat, A., Mcdonald, A.G., 2019. Pyrolysis Characterization and
43
44 comparison of pyrolysis products from fast pyrolysis of commercial *Chlorella vulgaris* and
45
46 cultivated microalgae. *J. Anal. Appl. Pyrolysis* 139, 258–273.
47
48
49 <https://doi.org/10.1016/j.jaap.2019.02.014>
50
51
52 [41] Suganya, T., Varman, M., Masjuki, H.H., Renganathan, S., 2016. Macroalgae and
53
54 microalgae as a potential source for commercial applications along with biofuels
55
56 production : A biore fi nery approach. *Renew. Sustain. Energy Rev.* 55, 909–941.
57
58
59
60
61
62
63
64
65

- 1
2
3
4 <https://doi.org/10.1016/j.rser.2015.11.026>
5
6
7 [42] Wang, K., Brown, R.C., Homsy, S., Martinez, L., Sidhu, S.S., 2013. Fast pyrolysis of
8
9 microalgae remnants in a fluidized bed reactor for bio-oil and biochar production.
10
11 Bioresour. Technol. 127, 494–499. <https://doi.org/10.1016/j.biortech.2012.08.016>
12
13
14 [43] Wang, X., Tang, X., Yang, X., 2017. Pyrolysis mechanism of microalgae *Nannochloropsis*
15
16 *sp.* based on model compounds and their interaction. *Energy Convers. Manag.* 140, 203–
17
18 210. <https://doi.org/10.1016/j.enconman.2017.02.058>
19
20
21 [44] Wang, Z., Li, H., Lim, C.J., Grace, J.R., 2018. Oxidative torrefaction of spruce-pine- fir
22
23 sawdust in a slot-rectangular spouted bed reactor. *Energy Convers. Manag.* 174, 276–287.
24
25 <https://doi.org/10.1016/j.enconman.2018.08.035>
26
27
28 [45] Yaman, O., Kulah, G., Koksall, M., 2019. Particuology Surface-to-bed heat transfer for high-
29
30 density particles in conical spouted and spout – fluid beds. *Particuology* 42, 35–47.
31
32 <https://doi.org/10.1016/j.partic.2018.03.013>
33
34
35 [46] Yang, C., Wang, C., Li, R., Zhang, B., Qiu, Q., Wang, B., Yang, H., Ding, Y., 2019.
36
37 Pyrolysis of microalgae : A critical review 186, 53–72.
38
39 <https://doi.org/10.1016/j.fuproc.2018.12.012>
40
41
42 [47] Yildiz, G., Lathouwers, T., Toraman, H.E., Geem, K.M. Van, Marin, G.B., Ronsse, F.,
43
44 Duren, R. Van, Kersten, S.R. a, Prins, W., 2014. Catalytic Fast Pyrolysis of Pine Wood : E
45
46 ff ect of Successive Catalyst Regeneration. *Energy & Fuels* 28, 4560–4572.
47
48 <https://doi.org/10.1021/ef500636c>
49
50
51 [48] Yu, Z., Dai, M., Huang, M., Fang, S., 2018. Catalytic characteristics of the fast pyrolysis of
52
53 microalgae over oil shale : Analytical Py-GC / MS study. *Renew. Energy* 125, 465–471.
54
55 <https://doi.org/10.1016/j.renene.2018.02.136>
56
57
58
59
60
61
62
63
64
65

1
2
3
4
5
6
7
8
9
10
11
12
13
14
15
16
17
18
19
20
21
22
23
24
25
26
27
28
29
30
31
32
33
34
35
36
37
38
39
40
41
42
43
44
45
46
47
48
49
50
51
52
53
54
55
56
57
58
59
60
61
62
63
64
65

[49] Yuan, T., Tahmasebi, A., Yu, J., 2015. Comparative study on pyrolysis of lignocellulosic and algal biomass using a thermogravimetric and a fixed-bed reactor. *Bioresour. Technol.* 175, 333–341. <https://doi.org/10.1016/j.biortech.2014.10.108>

[50] Zainan, N.H., Srivatsa, S.C., Li, F., Bhattacharya, S., 2018. Quality of bio-oil from catalytic pyrolysis of microalgae *Chlorella vulgaris*. *Fuel* 223, 12–19. <https://doi.org/10.1016/j.fuel.2018.02.166>

1
2
3
4
5
6
7
8
9
10
11
12
13
14
15
16
17
18
19
20
21
22
23
24
25
26
27
28
29
30
31
32
33
34
35
36
37
38
39
40
41
42
43
44
45
46
47
48
49
50
51
52
53
54
55
56
57
58
59
60
61
62
63
64
65

Figure captions

Figure 1. DTG curves of the three microalgae using a heating rate of 15 °C min⁻¹.

Figure 2. Main dimensions expressed in mm of the spouted bed reactor and its internals (fountain confiner and draft tube).

Figure 3. Product distribution obtained in the pyrolysis of microalgae NC, IG, TS at 500 °C.

Figure 4. Gaseous product composition obtained in the pyrolysis of NC, IG, TS at 500 °C.

Figure 5. Main compounds and their relative concentration in the bio-oils produced from the pyrolysis of NC, TS and IG

1
2
3
4
5
6
7
8
9
10
11
12
13
14
15
16
17
18
19
20
21
22
23
24
25
26
27
28
29
30
31
32
33
34
35
36
37
38
39
40
41
42
43
44
45
46
47
48
49
50
51
52
53
54
55
56
57
58
59
60
61
62
63
64
65

Table 1. Characteristics of the microalgae used in this study

	<i>NC</i>	<i>TS</i>	<i>IG</i>
Ultimate analysis (wt.%)^a			
C	44.45	43.54	48.35
H	6.50	6.76	7.24
N	7.75	7.33	7.60
O ^b	41.30	42.36	36.82
HHV (MJ/kg)	14.25	11.78	16.52
Proximate analysis (wt.%)			
Volatile matter	56.12	55.00	64.02
Fixed carbon	20.35	8.77	10.12
Moisture	2.00	3.36	2.27
Ash	21.51	32.86	23.56

^a ash free basis

^b calculated by difference

1
2
3
4
5
6
7
8
9
10
11
12
13
14
15
16
17
18
19
20
21
22
23
24
25
26
27
28
29
30
31
32
33
34
35
36
37
38
39
40
41
42
43
44
45
46
47
48
49
50
51
52
53
54
55
56
57
58
59
60
61
62
63
64
65

Table 2. Proximate and ultimate analyses of pyrolysis bio-chars.

	<i>NC</i>	<i>TS</i>	<i>IG</i>
Ultimate analysis^a			
C%	72.39	71.78	72.45
H%	4.47	3.66	3.38
N%	11.46	10.53	11.18
O% ^b	11.68	14.03	12.99
HHV (MJ/kg)			
Proximate analysis			
Volatile matter%	3.55	5.98	4.16
Fixed carbon%	21.25	30.44	26.70
Ash%	74.94	62.49	68.83

^a ash free basis

^b calculated by difference

1
2
3
4
5
6
7
8
9
10
11
12
13
14
15
16
17
18
19
20
21
22
23
24
25
26
27
28
29
30
31
32
33
34
35
36
37
38
39
40
41
42
43
44
45
46
47
48
49
50
51
52
53
54
55
56
57
58
59
60
61
62
63
64
65

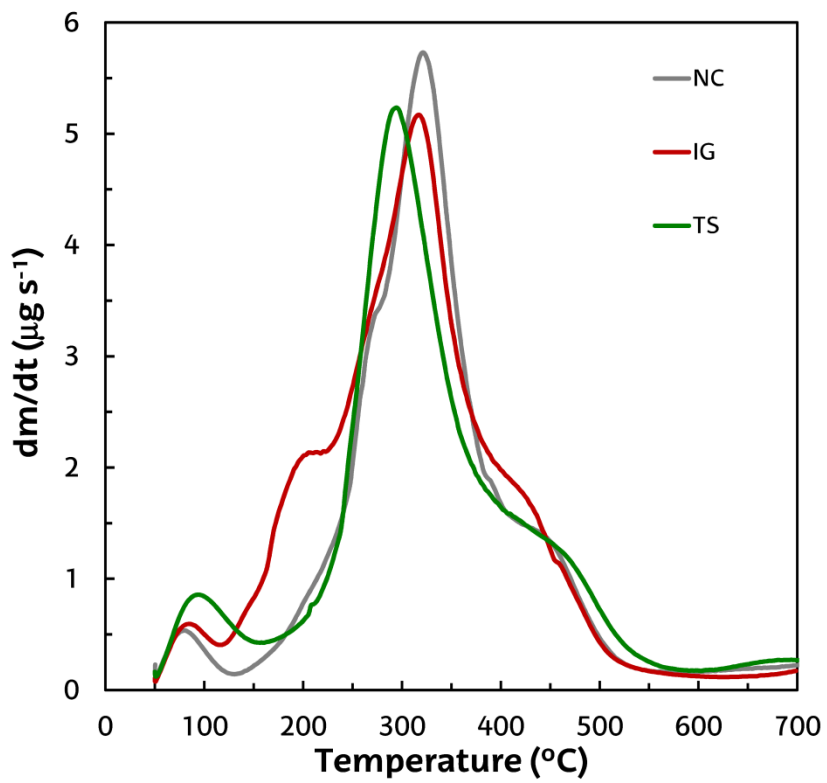


Figure 1.

1
2
3
4
5
6
7
8
9
10
11
12
13
14
15
16
17
18
19
20
21
22
23
24
25
26
27
28
29
30
31
32
33
34
35
36
37
38
39
40
41
42
43
44
45
46
47
48
49
50
51
52
53
54
55
56
57
58
59
60
61
62
63
64
65

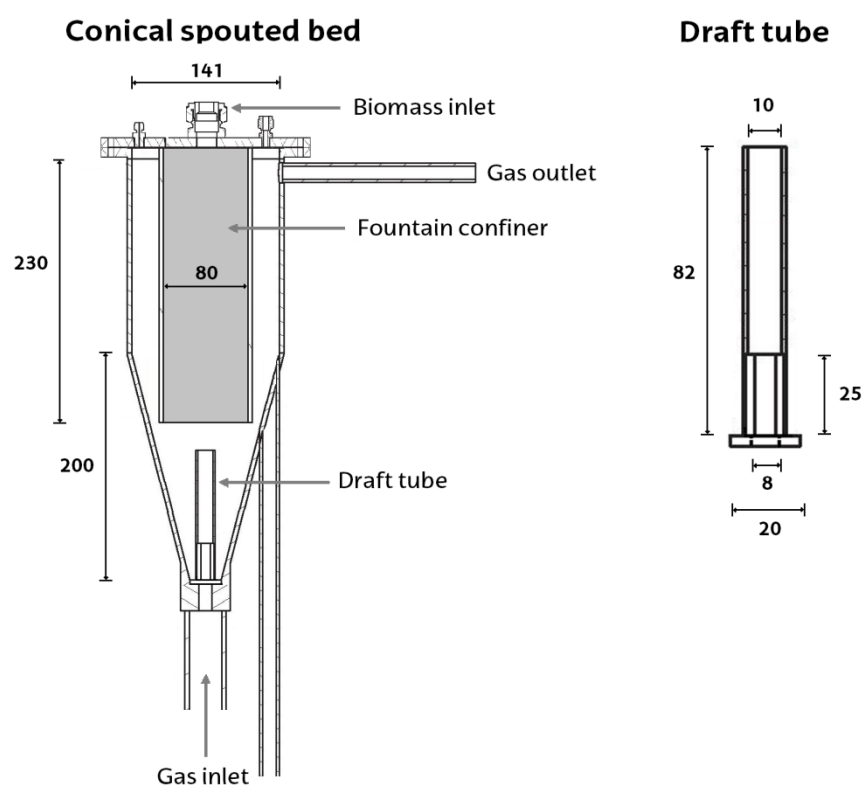


Figure 2.

1
2
3
4
5
6
7
8
9
10
11
12
13
14
15
16
17
18
19
20
21
22
23
24
25
26
27
28
29
30
31
32
33
34
35
36
37
38
39
40
41
42
43
44
45
46
47
48
49
50
51
52
53
54
55
56
57
58
59
60
61
62
63
64
65

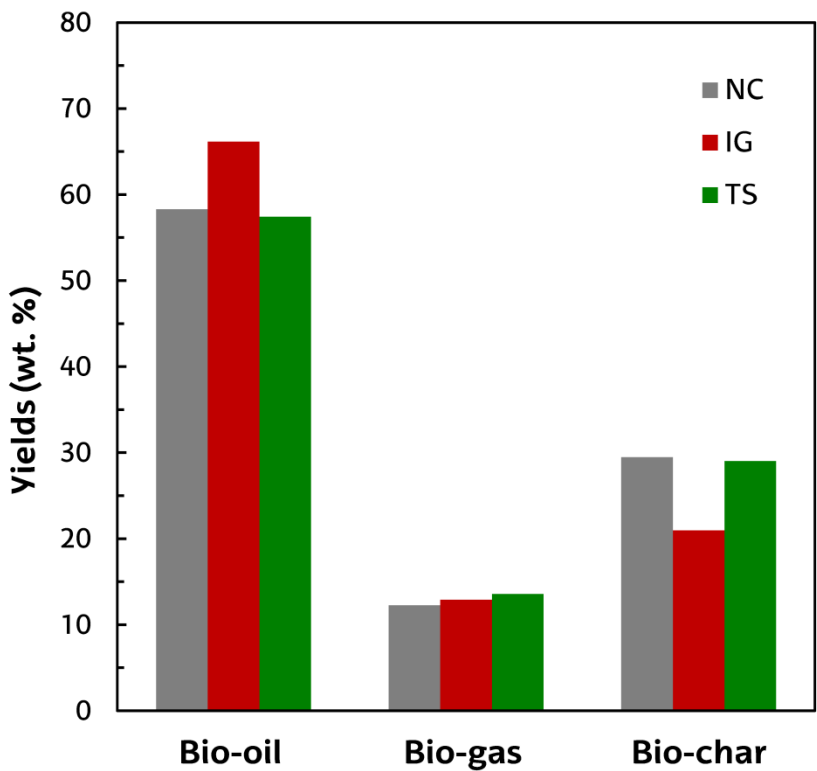


Figure 3.

1
2
3
4
5
6
7
8
9
10
11
12
13
14
15
16
17
18
19
20
21
22
23
24
25
26
27
28
29
30
31
32
33
34
35
36
37
38
39
40
41
42
43
44
45
46
47
48
49
50
51
52
53
54
55
56
57
58
59
60
61
62
63
64
65

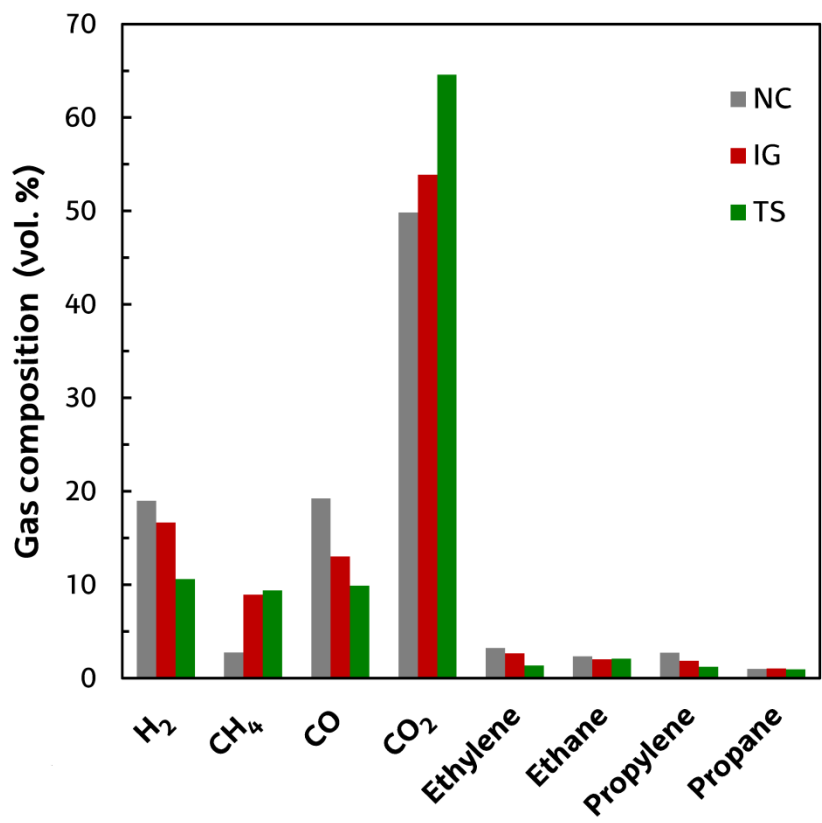


Figure 4.

1
2
3
4
5
6
7
8
9
10
11
12
13
14
15
16
17
18
19
20
21
22
23
24
25
26
27
28
29
30
31
32
33
34
35
36
37
38
39
40
41
42
43
44
45
46
47
48
49
50
51
52
53
54
55
56
57
58
59
60
61
62
63
64
65

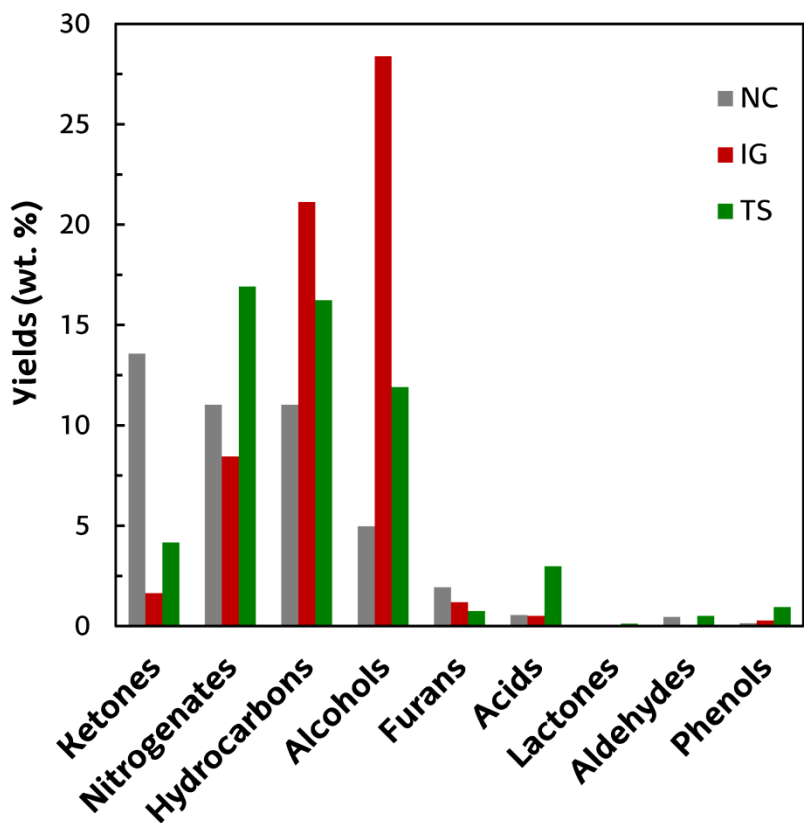


Figure 5.